Real-time fast ultrasonic monitoring of concrete cracking using embedded piezoelectric transducers

Cédric Dumoulin and Arnaud Deraemaeker

Université Libre de Bruxelles - BATir
50 av F.D. Roosevelt, CP 194/02
B-1050 Brussels, Belgium

E-mail: cedumoul@ulb.ac.be, aderaema@ulb.ac.be

Abstract. This paper deals with the use of embedded piezoelectric transducers for ultrasonic monitoring of cracking in concrete. Based on the previous developments of our research team on that topic, we design a new data acquisition system which is able to interrogate the emitter-receiver pair up to 150 times per second. The system is based on low-voltage actuation (up to 20 Volts) and the signal-to-noise ratio is excellent due to the use of a voltage amplifier at the receiver side and the possibility to perform averages. With such a high measurement rate, we are able to follow brittle failure events such as the failure of a concrete cylinder in compression, which is the application example presented. In this application, we show that, in addition to the ultrasonic active monitoring of cracking, the system is also able to record the passive acoustic emission events which can be used as a complementary indicator of damage in the cylinder. We also demonstrate that because of the high level of stresses in compression, the damage indicator defined in our previous studies is not suited for crack monitoring due to the elastoacoustic effect. The amplitude of the first wave arrival is shown to be a robust alternative damage indicator allowing to follow accurately the three successive phases of cracking leading to the failure of the cylinder.

Keywords: Embedded Transducers, PZT, Smart Aggregates, Concrete, Monitoring

Submitted to: *Smart Mater. Struct.*

1. Introduction

Concrete is the most widely used construction material in the world. It is used in many safety critical civil constructions such as bridges, dams, nuclear power plants, nuclear waste containers and skyscrapers, for which a permanent evaluation of the quality of the concrete is necessary to ensure safe and efficient maintenance. Current maintenance strategies are generally cost intensive and rely on scheduled manual inspections which are both impractical and insufficient. A great potential for optimizing maintenance exists through the implementation of on-line automated structural health monitoring (SHM) techniques.

The main cause for the loss of performance of concrete is cracking which initiates at the micro-scale, a scale smaller than the aggregates (<1cm), and much smaller than the structure. The typical size of a micro-crack is in the order of 10-100 microns. Automated SHM techniques using vibration based methods [1, 2] have been shown to be insensitive to such a small damage due to the low-frequency and global nature of the measured quantities, and are therefore not suited for early damage detection in concrete structures. An alternative is the use of local methods based on ultrasonic testing or acoustic emission [3, 4]. In our opinion, the main drawback of acoustic emission is the fact that if the monitoring system is down during the occurrence of cracking, the information is lost and cannot be recovered, whereas in ultrasonic testing, it is still possible to assess the state of damage afterwards even if the system has not been running during the cracking process.

For concrete structures, manual ultrasonic testing using external piezoelectric probes is a current practice described in the European Norm EN-12504-4 and the American Standard ASTM C597 02 (Standard Test Method for Pulse Velocity Through Concrete). There are however major drawbacks to this well established technique (i) the need of flat and accessible surfaces to place the external transducers, (ii) the use of coupling agent which reduces the efficiency of the transducers and (iii) the need for manpower to operate the device and hold the external transducers, which does not allow for on-line and real-time monitoring. In the last ten years, a few research groups, mainly in the US and in China have proposed to perform ultrasonic testing of concrete using low-cost embedded piezoelectric transducers instead of the bulky and expensive external probes. The main advantages of this technique are (i) an excellent coupling with the host structure without coupling agent, (ii) the flexibility in transducers arrangements, (iii) the fact that there is no need for manpower and that the monitoring can be performed on-line, and (iv) the protection of the embedded transducers from environmental and accidental attacks.

As the embedded transducers must act both as actuators and sensors, the best choice for the piezoelectric material is PZT (lead zirconate titanate). The acoustic im-

pedance of this material is however three times as large as the one of concrete so that wave transmission between the transducers and their surrounding is not optimal. Several research teams have therefore proposed to manufacture cement based piezoecomposites in order to produce transducers with a reduced impedance, matching closely the one of concrete. The composite can be achieved either by means of particles of piezoelectric material scattered in the cement matrix (0-3 composite) [5, 6], multiple PZT plates (2-2 composite) [7] or PZT rods (1-3 composite) [8, 9]. Although characterization of such composites has demonstrated the possibility to achieve impedance matching with the concrete, they cannot be embedded as such as they need to be waterproofed, electrically grounded and electromagnetically shielded. This requires extra layers which may affect the impedance matching negatively. 1-3 and 0-3 cement-based piezocomposites have been used for acoustic emission monitoring of cracking in [10, 11], and for active ultrasonic testing in [12]. An application of traffic monitoring monitoring using 1-3 composites is also reported in [13].

Another solution has been proposed in [14] which consists in embedding the bulk PZT in a waterproof coating, an electrically conductive layer acting as an electromagnetic shield, and a mechanically resistant material such as concrete or marble in order to protect the transducer during the casting process. The main advantage is the simplicity in the manufacturing process compared to piezocomposites, which leads to considerably lower costs. Such kinds of transducers have been successfully used for the monitoring of (i) cement and concrete hydration [15, 16], (ii) the evolution of the compressive strength of concrete at early age [14, 17], (iii) concrete cracking [18, 19, 20, 21, 22], (iv) water seepage [23, 24, 25] and (v) mechanical properties of concrete [26] including the acoustoelastic effect in compression [27]. All of these applications involve the use of active ultrasonic techniques where the transducers are used both as sensors and actuators. The major drawback of these transducers is the impedance mismatch with the host material (concrete), but recent research has shown that is was possible to optimize the wave transmission by a proper choice of the coating layers, and that impedance matching was actually not the main parameter to take into account to optimize the wave transmission when dealing with embedded transducers [28].

The transducers used in the present study are of the second category of embedded transducers with multiple coating layers. They have been designed and fabricated in the Civil Engineering laboratory at ULB-BATir and successfully used for the measurement of the P-wave velocity at early age [29], crack monitoring [30] and self-healing concrete monitoring [31]. In all of these applications, a short duration (5 μs) pulse excitation is sent to an emitter and the signal at the receiver side is recorded and post-processed in order either to extract the P-wave velocity, or to compute a damage indicator based on the first wave arrival. For crack monitoring, the main advantage of this technique is the possibility to perform fast interrogation: the signal recorded at the receiver has a length of about 3 to 5 ms which allows theoretically to measure at least 200 times per second

whereas techniques based on sweep sine excitations are much more time consuming. As it will be shown in this paper, measuring at such a high rate allows also to capture the acoustic events resulting from the cracking. Another advantage is the possibility to monitor on-line and in real-time brittle failure for non-reinforced concrete, which is the topic of the present study. Unfortunately, in our former applications, our commercial data acquisition system limited the number of possible measurements to one every 10 seconds and involved a high voltage (800 V) pulser at the emitter side, which is also limited in the rate at which it can send pulses due to its too slow rise-time.

This was the main motivation for developing a new flexible system which is presented in this study. The new system is low-voltage (10V for actuation) and allows to perform more than 150 measurements per second. Such a fast interrogation rate is important for two reasons: the first one is that it allows to perform averages on measurements and therefore to significantly increase the signal-to-noise ratio, and the second one is the possibility to monitor sudden cracking events.

Section 2 of this paper is devoted to the description of the newly developed fast crack monitoring system with embedded piezoelectric transducers. This newly developed monitoring system is applied for the crack monitoring of a cylinder in compression in Section 3. The study clearly shows that our former damage indicator is negatively impacted by the acoustoelastic effect [32] which could cause false alarms because the damage indicator is sensitive to both the early wave amplitude and the time of arrival, modified due to the acoustoelastic effect. This effect is discussed in Section 4 where an alternative damage indicator based on the amplitude of the first wave arrival is proposed.

The last section draws the conclusions and future research opportunities are outlined.

2. Fast crack monitoring system based on embedded piezoelectric transducers

The two main innovative elements of the crack monitoring system are the embedded transducers, and the fast interrogation unit, which are both described below.

2.1. Embedded transducers

The main element of the embedded transducers is a PZT patch of dimensions 12.5 x 12.5 x 0.2 mm. For several reasons such as the mechanical resistance and the electrical shielding, the PZT patch cannot be cast without coating layers. Since the fabrication of the first sensors [29, 30], many efforts in the manufacturing process have allowed to reduce drastically the electrical coupling between transducers and the electromagnetic interferences in comparison to other embedded piezoelectric transducers. Figure 1 shows the different material layers used during the manufacturing of the embedded transducers,

and a picture of the final transducer which is a disk of radius 20 mm and of thickness 8 mm. The waterproof coating is an epoxy resin.

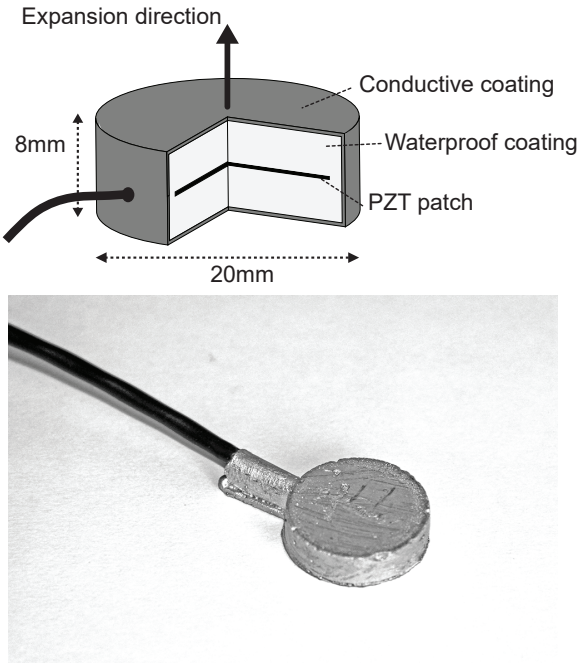

Figure 1. Embedded piezoelectric transducer, detail of the different layers

2.2. Fast data acquisition system

The aim of the current study is to detect the appearance of cracks and to continuously follow the level of damage of a concrete structure using ultrasonic measurements. The appearance of cracks or microcracks in concrete can be a very fast, random and brutal phenomenon. In order to follow each step of deterioration of concrete during the test, the number of measurements must be very large. A short pulse excitation signal has the advantage of exciting broadband frequencies in a short time. We have observed that in concrete, response signals to such excitations are generally totally attenuated after 3 to $5ms$. The new fast data acquisition system developed in this study is able to reach up to 150 ultrasonic measurements per second, which is close to the physical limit of about 200 measurements per second in order to avoid overlaps. The building blocks of the data acquisition system are: (i)the National Instruments NI-PXI-6115 data acquisition card, (ii) a laptop computer running the LABVIEW programming environment and linked to the acquisition card through a PCI Express port and (iii) a four channel high frequency (100Hz-1MHz) voltage pre-amplifier from SmartMote. Table 1 summarizes the properties of the acquisition system developed. In this study, The excitation signal is a low voltage short pulse ($5\mu s$, 10V). The duration of each measurement is $3ms$ which allows for a complete attenuation of the ultrasonic wave in the cylinder before the next measurement.

Table 1. Main properties of the fast ultrasonic measurement data acquisition system

Number of outputs	1 (4 MS/s)
Number of inputs	4 (10 MS/s)
Gain input	18 ... 60 dB
Output Signal	Arbitrary, up to 20V pp
Low-pass filter	100 Hz
High-pass filter	1 MHz
Measurement rate	up to 150 measurements/sec

We are able to achieve such a high sampling rate due to the fact that we are not using a high-voltage pulser (typically 400-800 V) as in most applications. The rise-time of a pulser is indeed too large in order to allow pulsing at such a high rate. Instead, we are using directly the 20 Volts output of the the NI-PXI-6115 card to excite the emitter. Because of this low-voltage actuation, we are using a pre-amplifier at the receiver side with an adjustable amplification factor from 18 to 60dB in a frequency band from 100Hz to 1MHz. The system is also designed to record average signal measurements with the goal of increasing the SNR (where the noise is due to the electronics in the data acquisition system). Its working principle is described in Figure 2.

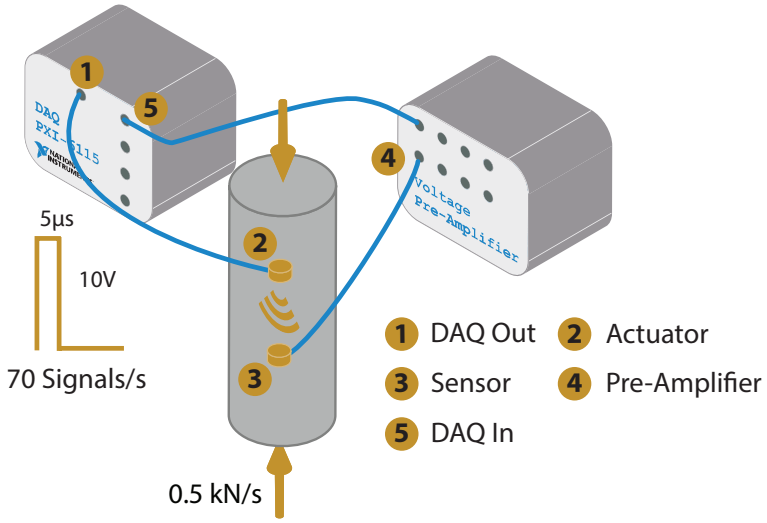

Figure 2. Fast and low-voltage data acquisition system for the monitoring of a concrete cylinder under uni-axial compression

3. Application

The experiment consists in a uni-axial compression test on a concrete cylinder (diameter 11.3 cm and height 22 cm). A pair of embedded transducers, distant of 15 cm, has been cast inside the cylinder (Figure 2). The concrete used for this experiment is an ordinary

concrete as described in Table 2. Six sixty millimeters strain gauges (SG) have been glued on the surface of the cylinder. Three have been placed for longitudinal strain measurement and three have been used for the measurement of the transversal strain (see Figure 3a). The SGs are located at 120° from each other. This eliminates the bending component from the strain measurements when the average is computed.

Table 2. Composition of the concrete used for the cylinder

Constituent	Density $[kg/m^3]$
Cement (CEM I 52.5 N PMES CP2)	340
Sand (Bernière 0/4)	739.45
Aggregates (Bernière 8/22)	1072.14
Water	184.22

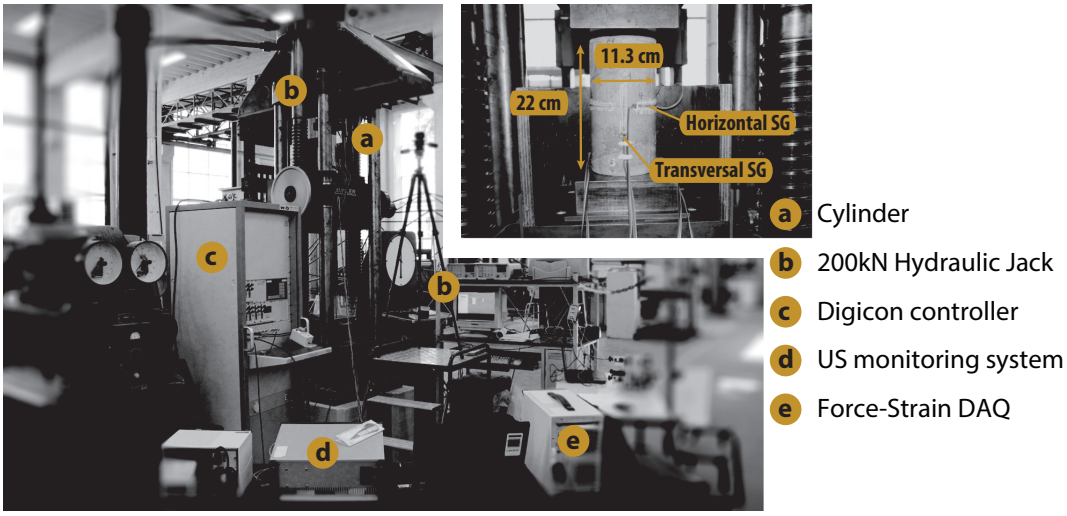

Figure 3. Overview of the test setup. The diameter of the cylinder is 11.3 cm and the height is 22 cm. The strain gauges are positioned at 120° from each other around the cylinder. The loading machine is a 1000 kN hydraulic jack controlled by a digital controller (Digicon).

The loading machine used for the experiment is a 1000kN hydraulic jack compression machine (see Figure 3). The machine is controlled by a digital controller (Digicon). The reaction of such machine is too slow and makes hazardous the measurement of the complete softening curve. Since the main goal of the test was to evaluate the evolution of the damage level with the load increase using ultrasonic techniques, it was decided to control the test in force. The loading rate has been fixed to 0.5 kN/s which corresponds (in the linear part) to a strain rate of 0.1 $10^{-3}/s$. This is an usual recommendation for uni-axial concrete tests. The force, the displacement and the strains have been recorded on a computer using a National Instruments DAQ system, respectively the NI PXI-4461 card for the displacement and the force measurements and

the NI PXIe-4330 card for the strain gauge measurements. The SGs have been wired with a quarter-bridge configuration. The ultrasonic measurement rate has been fixed to 70 measurements every second.

4. Test results

4.1. Strain gauge measurements

The stress-strain curves are given on Figure 4 (longitudinal strain) and Figure 5 (transversal strain). The values for each strain gauge (SG) and the mean value are shown both for the longitudinal and transverse strain measurements. After the linear region, one can observe a certain amount of dispersion between the different curves. This is mainly due to the non-symmetric appearance of damage due to initial weak zones [33]. The failure mechanism can be observed in Figure 6. It is a mixed mode between splitting (longitudinal cracks) and shear failure.

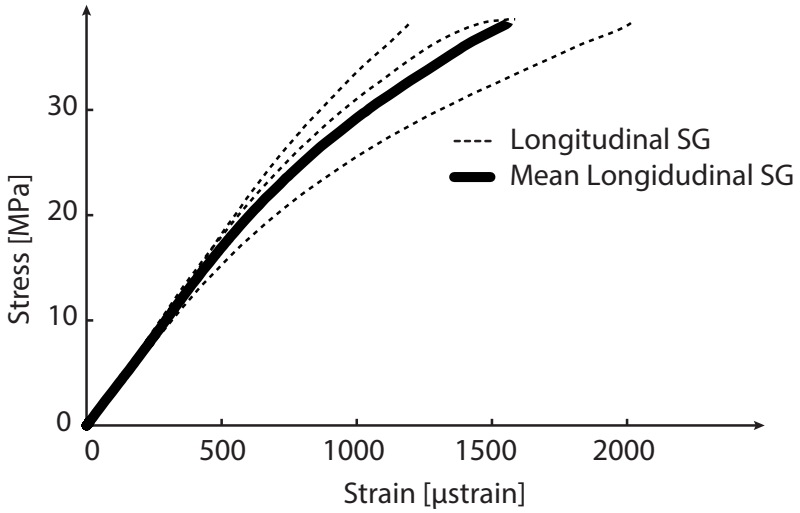

Figure 4. Longitudinal strain measured with 3 strain gauges disposed at 120° around the cylinder

4.2. Ultrasonic measurements

Because of the fast interrogation rate, the ultrasonic sensors pick-up both the signal generated by the emitter and the acoustic emission events due to the progressive cracking. These acoustic events must be detected for two reasons: (i) they need to be taken out of the measurements for the computation of the damage indicator, and (ii) they can be used independently for crack monitoring, as it will be demonstrated.

4.2.1. Acoustic emission events We have found that the amplitude of the acoustic emission events was of the same order of magnitude as the signals produced by the

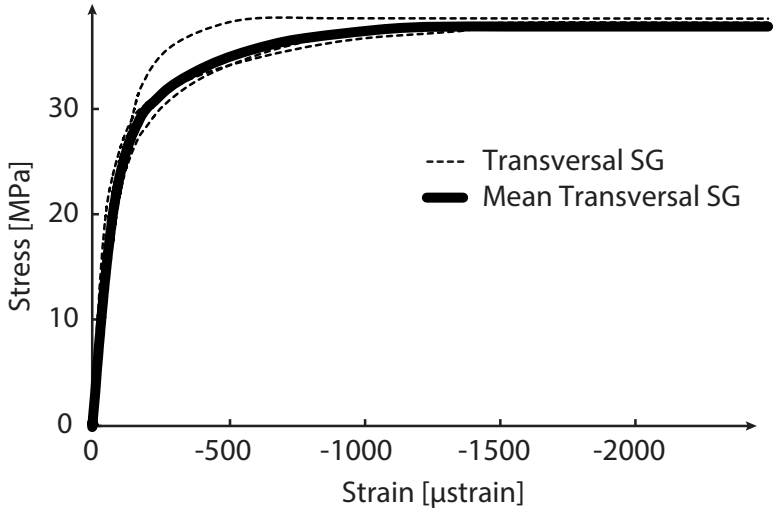

Figure 5. Transversal strain measured with 3 strain gauges disposed at 120° around the cylinder

Figure 6. Failure mechanism of the cylinder. The failure mode is a mixed mode between splitting and shear failure

monitoring system (Figure 7). As such, mixed signals cannot be used for crack monitoring. We propose here to identify the acoustic emission events by means of the difference of energy between the current signal measured and the average of the ten last sane measurements (without acoustic emission events). This is done by defining the following indicator:

$$AE_j = \frac{\int_0^{t_f} (x_j(t) - x_m(t))^2 dt}{\int_0^{t_f} x_m(t)^2 dt} \tag{1}$$

where $x_j(t)$ and $x_m(t)$ are respectively the j^{th} signal and the average of the last ten sane

signals. t_f is the measurement time (here 3 ms). This indicator is theoretically equal to 0 when the signal does not contain any acoustic emission event, and increases when an acoustic event is superimposed to the signal generated by the monitoring system. Because of the inevitable noise on the recorded signals, the indicator is not strictly equal to 0 for a sane signal. The threshold for the detection of acoustic emission events is therefore set to 0.1. In practice, the first ten sane signals are taken when no load is applied to the cylinder so that there are no acoustic emission events, and averaged. The value of AE is then computed for each new measurement and when the measurement is sane, it replaces the first measurement in the average of the ten sane signals.

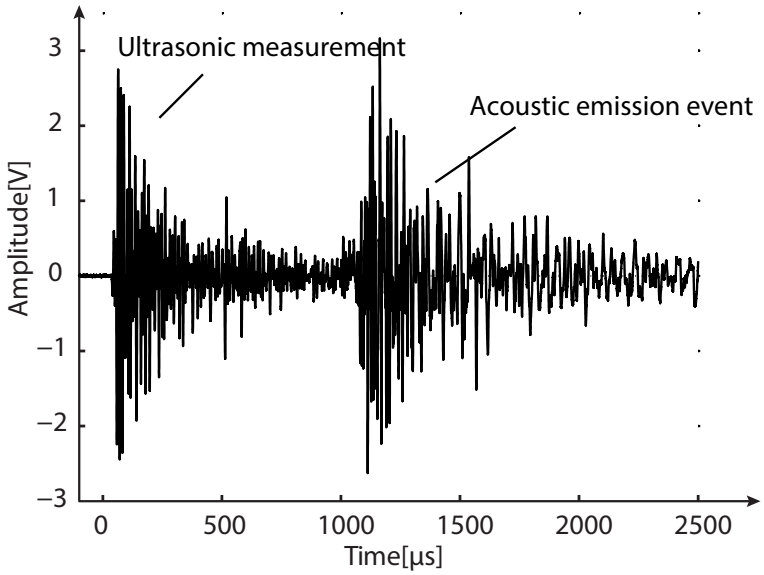

Figure 7. Mixture of signals coming from the monitoring system and from the fracture process. Both waves have an amplitude of the same order of magnitude.

The cumulative sum of the number of detected acoustic event is presented on Figure 8. It can be observed that the number of AE events grows exponentially in the non-linear part of the stress-strain curve. This is a usual result in acoustic emission monitoring, and demonstrates the fact that the developed sensors can also be used for acoustic emission testing. This is however not the scope of the present paper, and we will limit the study of the acoustic events to the cumulated sum of AE events.

4.2.2. Active ultrasonic crack monitoring Now that the signals polluted by the AE signals have been identified, we can apply the monitoring technique proposed in [30] in order to follow the cracking process of the concrete cylinder. The damage indicator is based on the simple reasoning that the first period of the recorded wave corresponds to the shortest wave path, which is affected only by the mechanical properties of the concrete between the transducers. This ensures that the crack monitoring is local, i.e. that the damage indicator will only react to cracking which occurs between the emitter

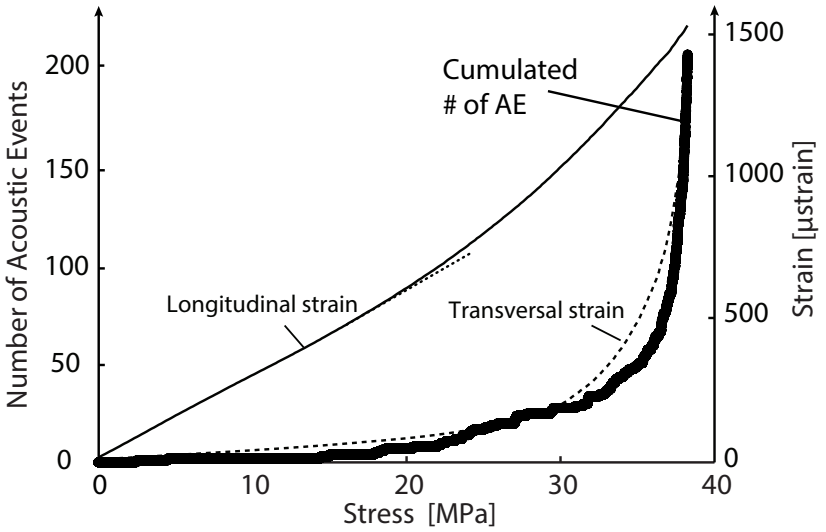

Figure 8. Evolution of the cumulated sum of AE events and compressive stress-strain curve

and the receiver. As a result, the waves which are reflected from the end surfaces of the cylinder are not polluting the measurement, as they arrive later in the signal.

The damage indicator is defined by the RMSD (Root Main Square Deviation) value between the healthy signal and a damaged signal computed in the time window corresponding to the first half-period of the undamaged signal:

$$I_j = \frac{\int_{t_1}^{t_2}(x_j(t) - x_0(t))^2 dt}{\int_{t_1}^{t_2} x_0(t)^2 dt} \tag{2}$$

where $x_j(t)$ and $x_0(t)$ are respectively the j^{th} signal and the original healthy (undamaged) signal. t_1 and t_2 correspond to the limits of the first half period of the healthy signal. This indicator is designed to react to a decrease of the wave velocity (increase of time of arrival) and of the amplitude of the first peak which happen when damage occurs. In such a case, its value should remain between 0 and 1. The evolution of the DI is shown in Figure 9.

The figure shows that the damage indicator reacts directly when the load is applied, which was unexpected, as it was never the case in previous studies. This damage indicator can therefore not be used for crack monitoring as it reacts to the loading before the appearance of damage an will cause false alarms in the monitoring system.

The most likely reason for this direct change is the acoustoelastic effect. The acoustoelastic effect states that the wave velocity changes as a function of the stress applied to the material. This effect has been shown to be important for concrete in compression due to the closing of voids or microcracks which stiffens the material locally. For a uniaxial test in the direction 1, the relationship between the velocity change and

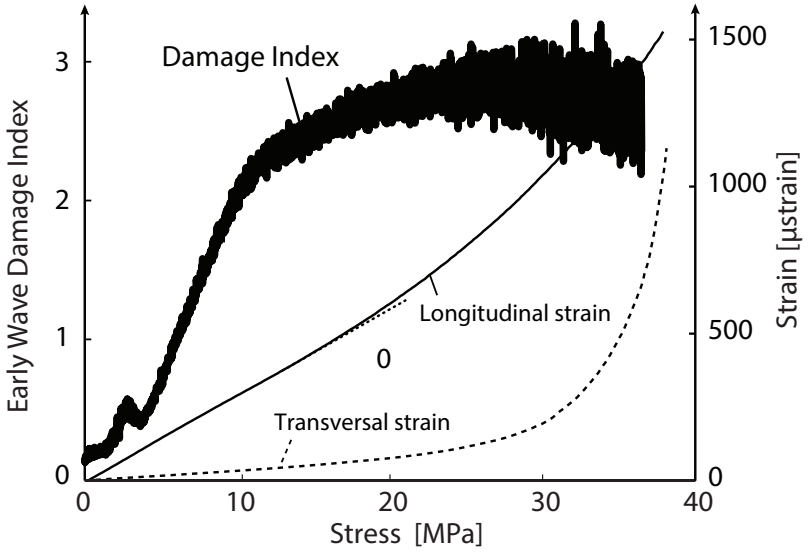

Figure 9. Evolution of the damage index and compressive stress-strain curve

the stress is given by [32] :

$$V_{ij} = V_{ij,0}(1 + A_{ij}\sigma_{11}) \tag{3}$$

where $V_{ij,0}$ is the velocity at zero stress for a wave polarized in direction j and traveling in direction i in a medium under uni-axial stress σ_{11} and A_{ij} are the acoustoelastic constants. In our case, we are measuring V_{11} (the wave velocity in the direction of the applied load) and previous studies have shown that the coefficient A_{11} is negative [32]: for a compression test, the stress is negative and the velocity increases with the level of stress. This is confirmed in Figure 10 where we plot the relative velocity change as a function of the stress level: below $10MPa$, the velocity increases up to a relative change of 3%. The shaded area represents the uncertainty in the estimation of the wave velocity, and the line represents an average value. There is a sudden drop of the velocity after $33MPa$ due to the fact that the first peak amplitude decreases so much that the estimation of time of flight is erroneous (it is based on the second peak instead of the first one).

Figure 9 also shows that the damage indicator does not remain between 0 and 1. This is due to the increase of velocity, which results in the difference of signals (green area in Figure 11) being greater than the reference signal in the period used for the computation of the indicator.

After the initial increase of the velocity, the damage induces a decrease of the average stiffness and, as a consequence, of the relative pulse velocity. We can see that the relative velocity is stabilized after $10MPa$ and decreases again near the failure. This behavior defines three different phases:

Phase I: The acoustoelastic effect results in an increase in the measured

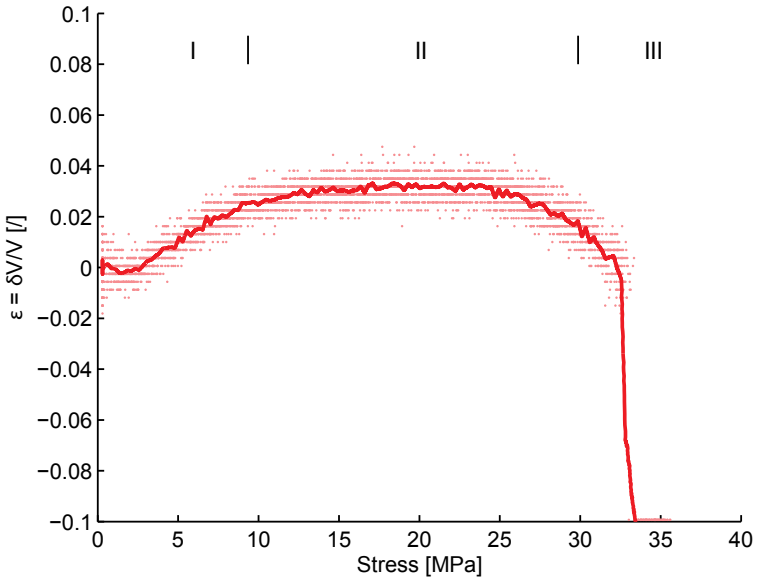

Figure 10. Evolution of the relative velocity with the compressive stress and stress-strain curve

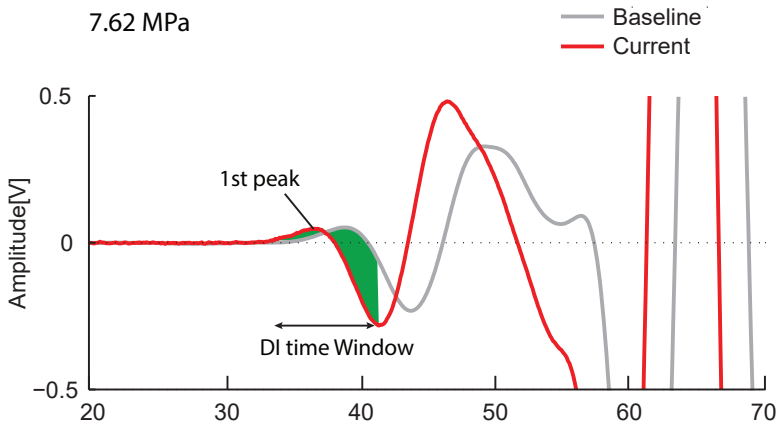

Figure 11. The damage indicator (DI) exceeds a value of one at a stress of $7.62MPa$ because of an increase of the velocity due to the acoustoelastic effect

velocities. The stress causes the closure of initial microcracks which leads to an increase in the stiffness and therefore the wave velocities. Appearance of damage (here in the form of new microcracks) results in a decrease of the wave velocities. Although the stress-strain curve seems to be linear it has been shown that microcracks appear when the external load is applied [33].

Phase II: Above $10MPa$, the velocity seems to be stabilized. There is a balance between the acoustoelastic effect which increases the velocity, and the damage which decreases it. During that phase, macrocracks parallel to

the load direction appear (Figure 6).

Phase III: At high level of load the whole cylinder is subjected to severe damage. It results in a fast decrease of the stiffness and therefore a decrease of the wave velocities which dominates the acoustoelastic effect, until the complete failure of the cylinder.

Because the wave velocity is sensitive to both the applied stresses and the damage, and because the order of magnitude of the two different phenomena is similar, the relative wave velocity change cannot be used to define the damage indicator. The damage indicator previously defined needs to be modified in order to be insensitive to the relative velocity change. This can be done by looking at the amplitude of the wave which is known to be sensitive to damage [34]. The amplitude of the first peak (defined in Figure 11) is represented in Figure 12. The figure shows that this alternative damage indicator is representative of the failure mechanism: below $5MPa$, the value is constant as the structure is undamaged. Between 5 and 10 MPa, the amplitude shows a sudden drop which is due to the onset of cracking. Note that at this stage, the stress-strain relationship is still linear, and the number of acoustic emission events is not significant enough to detect damage. This demonstrates the fact that ultrasonic waves are very sensitive to the cracking and can detect the onset of cracking before the macroscopic constitutive relation becomes non-linear, and before the cumulative sum of AE events becomes significant. After $10MPa$, the change of amplitude is slower due to the formation of the longitudinal cracks, and in the last phase, above $30MPa$, the decrease of amplitude is again faster until failure where the relative amplitude reaches a zero value.

Note that we did not notice any significant increase of the amplitude of the first peak due to the compressive stress. Such an effect of amplitude increase with compressive stress is indeed expected due to the closing of voids and microcracks [34] and can be observed in the present experiment on the following peaks (Figure 11). This effect should however be studied more carefully in the future..

5. Conclusion

In this study, a compression test has been performed on a concrete cylinder in which two embedded low-cost ultrasonic transducers have been cast in order to evaluate damage. The monitoring system developed allows to perform fast and on-line monitoring of concrete cracking (up to a measurement rate of 150 measurements per second) using low-voltage (10 V) short-pulse actuation. With such a high measurement rate, we have shown that acoustic emission events can also be detected, and we see this aspect as a promising feature for further developments of crack monitoring techniques based on our embedded transducers.

The test has shown that the acoustoelastic effect has a strong impact on the wave transmission in concrete when a high level of compressive stress is applied. It implies

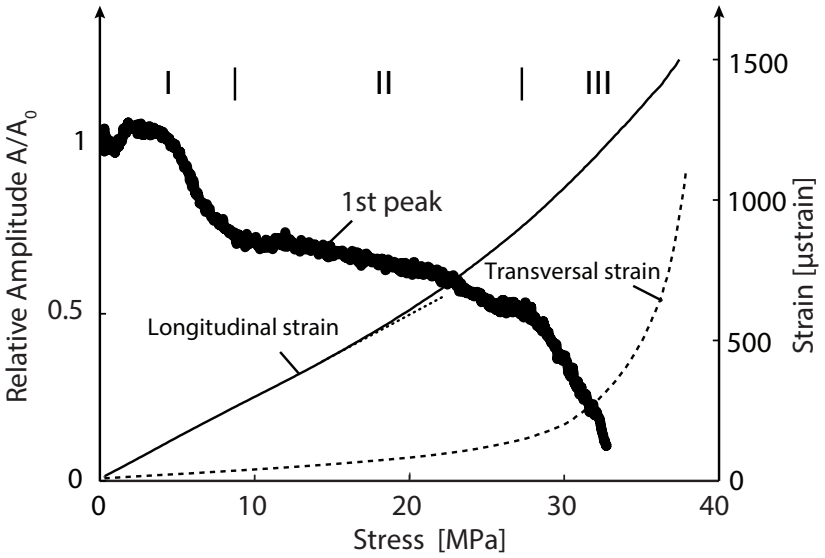

Figure 12. Evolution of the amplitude of the first peak with the compressive stress and stress-strain curve

that the previously defined damage index based on both the evolution of the wave velocity and the wave amplitude cannot be used since the effect of damage on the wave velocity cannot be distinguished from the acoustoelastic effect.

As an alternative, the amplitude of the first peak of the wave can be used. This indicator is interesting since it enables to follow accurately the three different phases which describe the failure mechanisms: microcracks initiation, appearance of longitudinal macrocracks, and complete failure. We have also shown that in this study, this indicator is more sensitive to cracking than counting the number of acoustic emission events. This finding still needs to be confirmed with further experiments.

An interesting future application of the monitoring system developed is to identify the acoustoelastic coefficients of concrete both in traction and compression. colorblue The impact of traction or compressive stresses on the wave amplitude should also be more carefully studied. Further developments of the system are foreseen in order to include a switching device enabling to interrogate multiple pairs of transducers successively, with potential applications to large scale concrete structures.

Acknowledgments

This study was supported by the Belgian National Fund for Scientific Research (FNRS) and by the Fonds Van Buuren.

References

[1] A. Deraemaeker and K. Worden. *New trends in vibration based structural health monitoring.* CISM Lecture Notes Vol 520. Springer, 2010.

[2] A. Deraemaeker, E. Reynders, G. De Roeck, and J. Kullaa. Vibration-based structural health monitoring using output-only measurements under changing environment. *Mech Sys. Sign. Proc.*, 22:34–56, 2008.

[3] C. Grosse and M. Ohtsu. *Acoustic Emission Testing.* Springer Berlin Heidelberg, Berlin, Heidelberg, 2008.

[4] M. Ohtsu. *Acoustic Emission and Related Non-destructive Evaluation Techniques in the Fracture Mechanics of Concrete: Fundamentals and Applications.* Elsevier Science, 2015.

[5] Z. Li, D. Zhang, and K. Wu. Cement-based 0-3 piezoelectric composites. *J. Am. Ceram. Soc*, 85(2):305–313, 2002.

[6] S. Huang, J. Chang, R. Xu, F. Liu, L. Lu, Z. Ye, and X. Cheng. Piezoelectric properties of 0-3 pzt/sulfoaluminate cement composites. *Smart Mater. Struct.*, 13:270–274, 2004.

[7] B. Dong and Z. Li. Cement-based piezoelectric ceramic smart composites. *Composites Science and Technology*, 65:1363–1371, 2005.

[8] K.H. Lam and H.L.W. Chan. Piezoelectric cement-based 1-3 composites. *Applied Physics A*, 81:1451–1454, 2005.

[9] Z. Li, S. Huang, L. Qin, and X. Cheng. An investigation on 1-3 cement based piezoelectric composites. *Smart Mater. Struct.*, 16:999–1005, 2007.

[10] Y. Lu, Z. Li, and W.I. Liao. Damage monitoring of reinforced concrete frames under seismic loading using cement-based piezoelectric sensor. *Materials and Structures*, 44:1273–1285, 2011.

[11] L. Qin, S. Huand, X. Cheng, Y. Lu, and Z. Li. The application of 1-3 cement-based piezoelectric transducers in active and passive health monitoring for concrete structures. *Smart Mater. Struct.*, 18, 2009. 095018.

[12] L. Qin, S. Huang, X. Cheng, Y. Lu, and Z. Li. The application of 1-3 cement-based piezoelectric transducers in active and passive health monitoring of concrete structures. *Smart Mater. Struct.*, 18, 2009. 095018.

[13] J. Zhang, Y. Lu, Z. Lu, C. Liu, G. Sun, and Z. Li. A new smart traffic monitoring method using embedded cement-based piezoelectric sensors. *Smart Mater. Struct.*, 24, 2015. 025023.

[14] H. Gu, G. Song, H. Dhonde, Y.L. Mo, and S. Yan. Concrete early-age strength monitoring using embedded piezoelectric transducers. *Smart Mater. Struct*, 15:1837–1845, 2006.

[15] L. Qin and Z. Li. Monitoring of cement hydration using embedded piezoelectric transducers. *Smart Mater. Struct.*, 17, 2008. 055005.

[16] Q. Kong, S. Hou, Q. Ji, Y.L. Mo, and G. Song. Very early age concrete hydration characterization monitoring using piezoceramic based smart aggregates. *Smart Mater. Struct.*, 22, 2013. 085025.

[17] W. Dansheng and Z. Hongping. Monitoring of strength gain of concrete using embedded PZT impedance transducer. *Construction and Building Materials*, 25:3703–3708, 2011.

[18] G. Song, H. Gu, Y.L. Mo, T.T.C. Hsu, and H. Dhonde. Concrete structural health monitoring using embedded piezoceramic transducers. *Smart Mater. Struct.*, 16:959–968, 2007.

[19] X. Zhao, H. Li, D. Du, and J. Wang. Concrete structure monitoring based on built-in piezoelectric ceramic transducers. *Proc of SPIE Vol 6932, 693208*, 2008.

[20] V.G.M. Annamdas, Y. Yang, and C.K. Soh. Impedance based concrete monitoring using embedded PZT sensors. *Int. J. Civil and Struct. Engng*, 1(3):414–424, 2010.

[21] W.I. Liao, J.X. Wang, G. Song, H. Gu, C. Olmi, Y.L. Mo, K.C. Chang, and C.H. Loh. Structural health monitoring of concrete columns subjected to seismic excitations using piezoceramic-based sensors. *Smart Mater. Struct.*, 20, 2011. 125015.

[22] Q. Feng, Q. Kong, L. Huo, and G. Song. Crack detection and leakage monitoring on reinforced concrete pipe. *Smart Mater. Struct.*, 24, 2015. 115020.

[23] D. Zou, T. Liu, Y. Huang, F. Zhang, C. Du, and B. Li. Feasibility of water seepage monitoring in concrete with embedded smart aggregates by P-wave travel time measurement. *Smart Mater. Struct.*, 23, 2014. 067003.

[24] Q. Kong, Q. Feng, and G. Song. Water presence detection in a concrete crack using smart aggregates. *Int. J. of Smart and Nano Mat.*, 6(3):149–161, 2015.

[25] Tiejun Liu, Yongchao Huang, Dujian Zou, Jun Teng, and Bo Li. Exploratory study on water seepage monitoring of concrete structures using piezoceramic based smart aggregates. *Smart Materials and Structures*, 22(6):065002, 2013.

[26] Z. Li, L. Qin, and S. Huang. Embedded piezo-transducer in concrete for property diagnosis. *Journal of Materials in Civil Engineering*, 21(11), 2009. 085025.

[27] Tiejun Liu, Dujian Zou, Chengcheng Du, and Ying Wang. Influence of axial loads on the health monitoring of concrete structures using embedded piezoelectric transducers. *Structural Health Monitoring*, 16(2):202–214, 2017.

[28] C. Dumoulin and A. Deraemaeker. Design optimization of embedded ultrasonic transducers for concrete structures assessment. *Ultrasonics*, 79:18–33, 2017.

[29] C. Dumoulin, G. Karaiskos, J. Carette, S. Staquet, and A. Deraemaeker. Monitoring of the ultrasonic P-wave velocity in early-age concrete with embedded piezoelectric transducers. *Smart Mater. Struct.*, 21, 2012. 047001.

[30] C. Dumoulin, G. Karaiskos, J.Y. Sener, and A. Deraemaeker. On-line monitoring of cracking in concrete structures using embedded piezoelectric transducers. *Smart Mater. Struct.*, 23(11), 2014. 115016.

[31] E. Tsangouri, G. Karaiskos, D.G. Aggelis, A. Deraemaeker, and D. Van Hemelrijck. Crack sealing and damage recovery monitoring of a concrete healing system using embedded piezoelectric transducers. *Structural Health Montoring*, 2015. 1475921715596219.

[32] I. Lillamand, J.J. Chaix, M.A. Ploix, and V. Garnier. Acoustoelastic effect in concrete material under uni-axial compressive loading. *NDT & E International*, 43:655–660, 2010.

[33] J.G.M Van Mier. *Fracture Processes of Concrete - Assessment of Material Parameters for Fracture Models*. CRC Press, 1996.

[34] W. Suaris and V. Fernando. Ultrasonic pulse attenuation as a measure of damage growth during cyclic loading of concrete. *ACI Mater. J.*, 84(3):185–193, 1987.